



UNIVERSITY OF LEEDS

This is a repository copy of *Backcalculation of pavements incorporating Grouted Macadam technology*.

White Rose Research Online URL for this paper:
<http://eprints.whiterose.ac.uk/115824/>

Version: Accepted Version

Article:

Požarycki, A, Fengier, J, Górnaś, P et al. (1 more author) (2018) Backcalculation of pavements incorporating Grouted Macadam technology. *Road Materials and Pavement Design*, 19 (6). pp. 1372-1388. ISSN 1468-0629

<https://doi.org/10.1080/14680629.2017.1310668>

© 2017 Informa UK Limited, trading as Taylor & Francis Group. This is an Accepted Manuscript of an article published by Taylor & Francis in *Road Materials and Pavement Design* on 17 April 2017, available online:

<https://doi.org/10.1080/14680629.2017.1310668>. Uploaded in accordance with the publisher's self-archiving policy.

Reuse

Items deposited in White Rose Research Online are protected by copyright, with all rights reserved unless indicated otherwise. They may be downloaded and/or printed for private study, or other acts as permitted by national copyright laws. The publisher or other rights holders may allow further reproduction and re-use of the full text version. This is indicated by the licence information on the White Rose Research Online record for the item.

Takedown

If you consider content in White Rose Research Online to be in breach of UK law, please notify us by emailing eprints@whiterose.ac.uk including the URL of the record and the reason for the withdrawal request.



eprints@whiterose.ac.uk
<https://eprints.whiterose.ac.uk/>

Backcalculation of pavements incorporating grouted macadam technology

Andrzej Pożarycki^a, Jakub Fengier^a, Przemysław Górnaś^a, Dariusz Wanatowski^a

^aInstitute of Civil Engineering, Poznan University of Technology, Poland; ^bSchool of Civil Engineering, Faculty of Engineering, University of Leeds, United Kingdom

ARTICLE HISTORY

Compiled February 13, 2017

ABSTRACT

Applying cement grout with a high compressive strength to a porous layer made of asphalt concrete results in a pavement with the properties of an intermediate type that combines the characteristics of both flexible and rigid pavements. This solution is known as Grouted Macadam. Despite a wide range of test results on the GM pavements presented in the literature, there are very few advanced modelling solutions formulated in the scope of bearing capacity measured in-situ by means of a Falling Weight Deflectometer. This paper turns out that the seemingly small frequency of loading (≈ 20 Hz) generated during pavement deflection measurements using a Falling Weight Deflectometer - like device, has a significant impact on the backcalculation results of grouted macadam pavements. The study shows that, introducing frequency normalisation of both the pavement loading and vertical displacements to the backcalculation, can limit the statistical scatter of backcalculation results by close to a half in comparison with the classical backcalculation procedure.

KEYWORDS

Grouted macadam; flexible pavement; backcalculation; quasi-static; deflection basin

1. Introduction

Applying cement grout with a high compressive strength to a porous layer made of asphalt concrete (AC) results in a pavement with the properties of an intermediate type that combines the characteristics of both flexible and rigid pavements. This solution is known as Grouted Macadam (GM). The GM layer is generally described as an open-graded asphalt concrete mixture containing from 25 to 35% air voids, which are filled with a resin-modified Portland cement grout. The GM technology provides several advantages to a pavement, including a high resistance to permanent deformations, high compressive strength, light colour and the lack of requirement for cutting expansion joints (in comparison to the traditional rigid pavements).

Numerous studies have been carried out on the GM pavements in the last two decades. Most of them were focused on the analysis of various physical and mechanical characteristics of the GM pavements including compressive strength (Anderton, 2000; Collop & Elliott, 1999; Oliveira, 2006; Setyawan, 2006), flexural strength (Anderton, 2000; Oliveira, 2006), fatigue strength (Collop & Elliott, 1999; Oliveira, 2006),

or thermal expansion coefficient described by Anderton (2000). Furthermore, Oliveira (2006) carried out large – scale tests showing a significant rutting resistance of the pavement with a GM layer. Anderton (2000) reported that anti-skid properties of the GM layer (named there also as "resin modified pavement") were equivalent to the standard pavement requirements in the US. Oliveira (2006) and (Oliveira, Salah, Thom, & Pereira, 2007) also proposed a design procedure for pavements incorporating GM layers. Some researchers pointed out several challenges associated with modelling such pavement courses. It has been proven that it is adequate to use advanced modelling solutions for describing the behaviour of the flexible pavement structures with the granular aggregate base and a thin AC layer. (Al-Qadi, Wang, & Tutumluer, 2010; Papadopoulos & Santamarina, 2015) suggested using the cross anisotropy and stress – dependent constitutive model in order to achieve satisfying results from a three – dimensional finite element method. Bianchini (2014), on the other hand, emphasised the lack of the fatigue criteria for the GM pavements.

Despite a wide range of test results on the GM pavements presented in the literature, there are a relatively few conclusions formulated in the scope of bearing capacity of those solutions in-situ (e.g. using Falling Weight Deflectometers - FWDs). In general, the analysis of the pavement test results using FWD devices is a well – established topic in the literature (Garbowski & Pożarycki, 2016; Guzina & Osburn, 2002; Sangghaleh et al., 2013; SHRP, 1993; Ullidtz & Coetzee, 1995; Westover & Guzina, 2007; Yi & Mun, 2009). However, this technique belongs to the group of so – called backcalculation methods, which are intrinsically poorly conditioned in the mathematical sense. Consequently, the unambiguity of calculation results is affected by backcalculation sensitivity to the shape of pavement deflection curves (Sangghaleh et al., 2013), compensation effect or incorrectly determined thickness of the pavement courses (Ceylan, Gopalakrishnan, Bayrak, & Guclu, 2013). According to Ullidtz and Coetzee (1995), compensation effect known also as "a compensating layer and non-linear effects" is an effect that essentially results from incorrect modelling of the pavement material response and the sequential nature of the backcalculation iterative procedure, as well as the geometry of a deflection basin test. A typical result may show, as an example, subgrade modulus that is significantly higher than expected for the material type, while the base layer modulus is far too low and the surfacing modulus is too high. For instance, the authors' experience showed that changing the thickness of the upper pavement layers by 6% influences the values of their determined stiffness moduli by 46%. Similar conclusions were also reported by other researchers (e.g. Irwin, Yang, and Stubstad (1989)).

The thickness of the layer constructed using the GM technology is usually assumed in a range of 4 to 6 cm. It needs to be pointed out that the backcalculation requires the thickness of layer in a pavement model to be equal to at least half of the radius of the agreed circular loaded area Ullidtz and Coetzee (1995) (that is 7.5 cm using a standard FWD loading plate). Since the applied thickness of GM layers does not fulfil this condition, the task formulated in this way is related to pavement modelling issues with the so-called thin layer (SHRP, 1993; Von Quintas, Bush, & Baladi, 1994; Von Quintus & Killingsworth, 1997).

The loads that act on the road pavements are cyclic loads or repeated loads. Duration of a single load impulse (equal to the sum of load increment time and load reduction time) due to a single pass of a truck wheel travelling with a speed of 50 km/h, is approximately equal to 0.02 s. Thus, the frequency of the pavement load is about 20 Hz. Considering the definition of static load ($f = 0$ Hz), any frequency of a single load impulse implies the presence of inertial forces. In this context, both cyclic

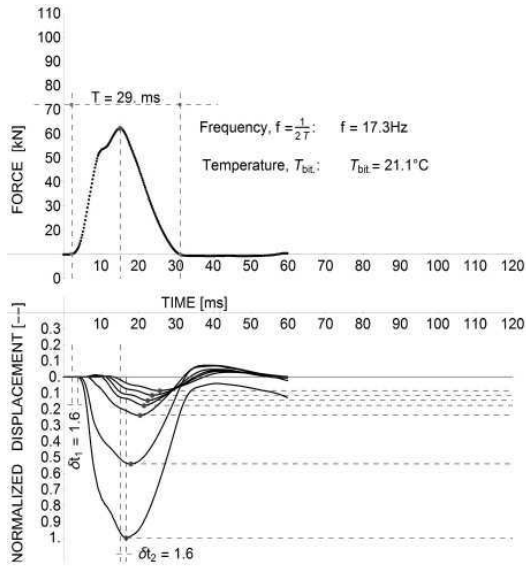
and repeated loads, can be considered as dynamic loads acting on the road pavements. Therefore, as a result of dynamic loading, the most natural way of modelling pavement mechanics is using a model which takes into account dynamic effects. In general, it is possible to use a pavement model based on the Layer Elastic Theory (LET) expressed with a dynamic system of equations Wozniak (1996) or spectral elements approach (Al-Khoury, Scarpas, Kasbergen, & Blaauwendraad, 2001). Notwithstanding the use of the method, dynamic loading conditions entail the necessity of applying a larger number of layer parameters compared to a system of equations on the assumption of static loading conditions. In a LET static model, the number of parameters required for the definition of a single layer is limited to three: thickness, elasticity modulus, and Poisson's ratio. In consequence, whenever there are no reliable data, the solution of the task is reduced to a static model and a deflection curve, which is often referred to as the Classical Deflection Curve (CDC). Such a solution is combined of maximum values of both the registered displacement function, as well as the load function. The drawback of reducing the dynamic equations to a form in which the influence of dynamic loads is omitted, is an inconsistency between a static loading model, and the dynamic nature of load in the FWD test, which is why it is worth looking for intermediate methods.

Whenever asphalt layers and the layer made of GM are treated as a single layer in a computer model of pavement, the commonly used backcalculation logic of merging layers with similar stiffnesses becomes disrupted. Although the asphalt and GM layers have different physical and mechanical properties, the GM layer is only 5 cm thick. Thus, according to the backcalculation criteria quoted above, it constitutes a thin layer.

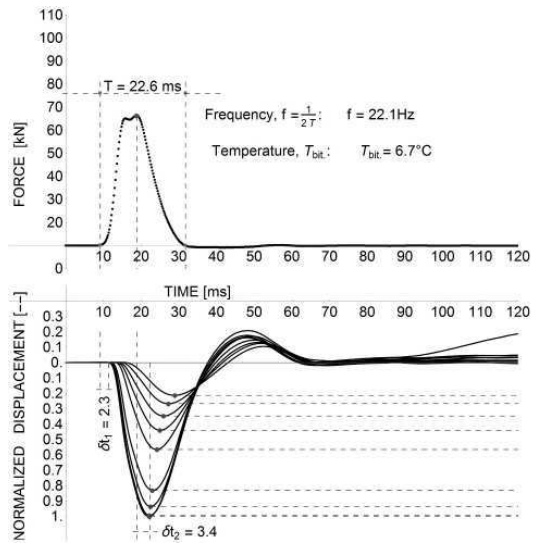
The aim of this paper is to verify a method of frequency normalisation for both the functions of load and displacements, based on the pavement deflection measurements from the FWD device. The calculation results obtained from the new method are characterised by a lower statistical scatter in comparison with a range of values obtained without using such a normalisation.

2. Methods

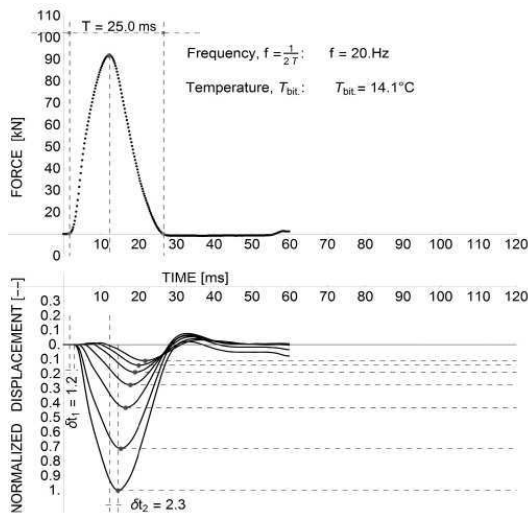
A deflection curve, which is the result of the analysis of vertical displacements measured on the roadway's surface in different distances from the load axis, is commonly used in the standard backcalculation of pavement layers. Those displacement values can be obtained either from the FWD measurements or their simulations. As far as pavement measurement results from the dynamic impact loading of the FWD type are concerned, the results come in a set of $F(t)$, $u_r(t)$ values, which are the force and displacements in the function of time (where the subscript r is the distance from the load axis). A few examples of the FWD measurement results obtained for different types of pavements are illustrated in Fig. 1, which shows that both the frequency of the load (f) and displacement functions are not constant quantities.



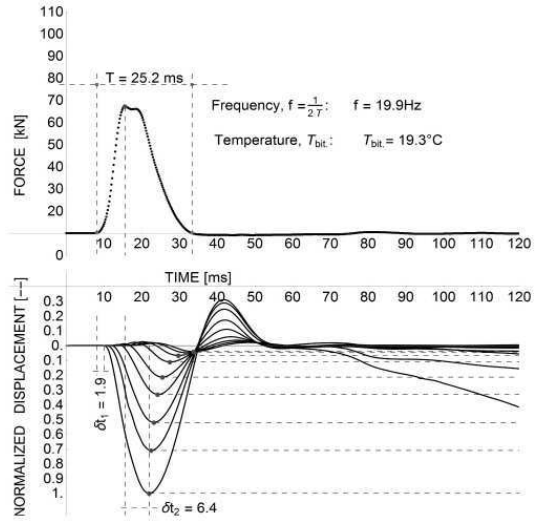
(a) Flexible pavement.



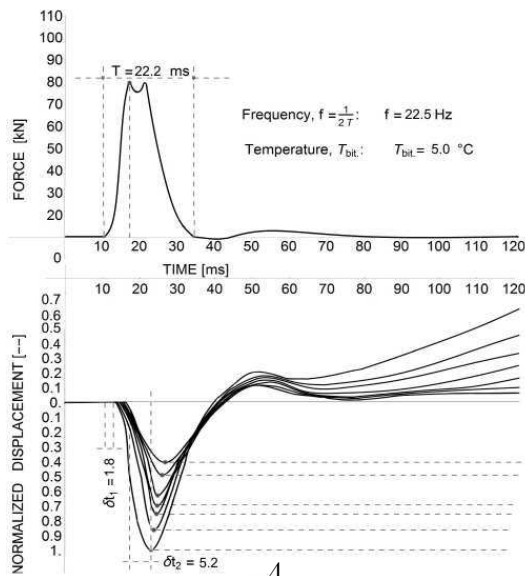
(b) Pavement with three HMAC layers.



(c) Pavement with one, thin HMAC layer.



(d) Semi-rigid pavement



(e) Pavement with a GM layer.

Figure 1. Examples of normalised results obtained using FWD device for different pavement structures (the abbreviation HMAC stands for high modulus asphalt concrete).

3. Two – step normalisation of FWD signals

A more accurate approach to constructing a deflection curve in backcalculation (compared to the classical deflection curve) is the frequency normalisation of the load and deflection functions. In such a case the calculations cover the dynamic part of the FWD test and the static model for backcalculation can be used. For instance, this idea was used by Kang (1998) and Guzina and Osburn (2002). They have shown that, by the application of signal theory, the values of load and displacement determined in time domain can be reduced to frequency domain using the Fourier transform.

3.1. Step one, selecting the best method of data pre-processing

A detailed analysis of the results reported by Westover and Guzina (2007) and well as authors' own experience in analysing various pavement structures, show that the normalisation method based on the fast Fourier transform (FFT) operator, is relatively sensitive to the shape of the signals generated from in-situ measurements. It is also well known that the Fourier transform assumes the processed time function $g(t)$ should be a continuous and periodic function. However, the deflection measurement functions are often discontinuous. The concept of discontinuity for deflection surface measurements in confrontation with the assumptions of the Fourier transform is illustrated in Fig. 2 (assuming that $g(t)$ can be either the displacement or loading in the function of time, as shown in Fig. 1).

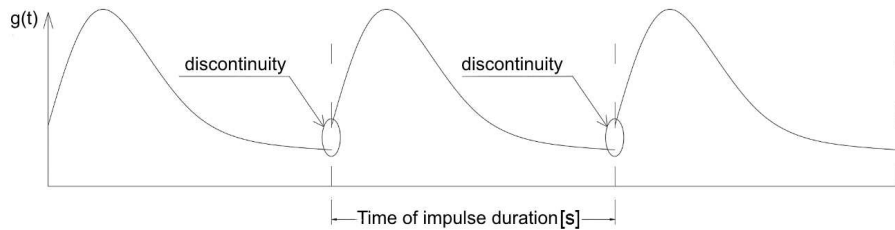


Figure 2. Discontinuity for repeated signals, which is both undesirable for fast Fourier transform operator and typical for pavement deflection measurements by using FWD – type device.

In the case of discontinuity, the calculation of the amplitude spectrum (the function of displacements in the frequency domain) discloses so-called the spectral leakage, which effectively interferes with the inverse calculation results. It is possible to reduce the impact of the spectral leakage for a certain group of pavement deflection results obtained from the FWD, by extending the time recording movements during measurement (e.g. from 60 ms to 120 ms), until the full dumping vibration of the pavement is achieved. However, in the tests performed in the present study, there have been many cases for which the procedure has not brought satisfactory improvements (e.g. Fig. 1e). It was noted that the adverse effect of spectral leakage concerns mainly the pavement with relatively thin layers and functions of displacement obtained in close proximity to the load axis (the first two displacement transducers, located in the load axis and 30 cm from it). As a result, unlike in the case of pure synthetic data analysis reported by Guzina and Osburn (2002), the real measurement signals usually require additional transformation. Random noise inherent to the transducers and data collection system is accumulated during this integration resulting in a non-zero displacement at the end of the record known as baseline offset. According to Westover and Guzina (2007),

this leads to significant errors in the frequency – based interpretation. It is therefore necessary to account for this non-zero displacement with a proper baseline correction (bc) given by Eq. (1).

$$u_k^{bc}(t_j) = u_k(t_j) - \frac{u_k(t_M) - u_k(t_0)}{(t_M - t_0)^n} \cdot (t_j)^n \quad (1)$$

where:

$u_k^{bc}(t_i)$ – geophone displacement record and corresponding time – history t_i
 n – is the power of the baseline correction,
 k – in the number of geophone.

All this leads to the backcalculation method that must be preceded by pre-processing of signals registered during the in-situ measurements. In the current study, the assumed sampling frequency of the signals obtained during the FWD test (equal to 20 kHz) was increased to 2000 kHz (by means of interpolation) and all the signals were then pre-processed prior to the Fourier transform using the following methods:

Method no. 1: The duration of $F(t)$ and $u_r(t)$ source signals were subject to modifications. It is assumed that only a pure signal from range of $t \in \langle 0, 60 \rangle$ [ms] is taken into consideration (the spectral leakage is admissible). First registered value by FWD measurement software equals to the signal beginning.

Method no. 2: Analogical to the method no. 1; however, a longer signal time is used in calculations $t \in \langle 0, 120 \rangle$ [ms].

Method no. 3: The source signals from measurements are modified according to the assumptions that $F(t \leq t_{1f}) = 0$, $F(t \geq t_{2f}) = 0$, $u_r(t \leq t_{1ur}) = 0$, $u_r(t \geq t_{2ur}) = 0$ (the source signals start and end with zero value). The scheme of this modification is shown in Fig. 3.

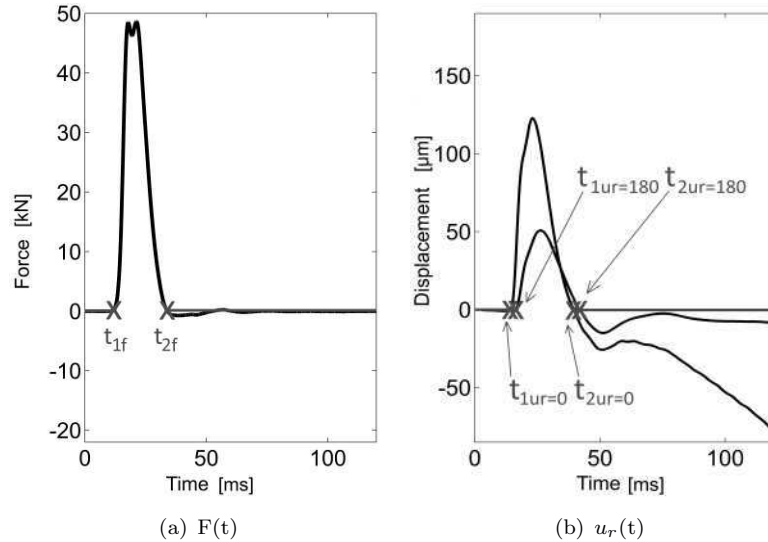


Figure 3. The diagrams of the source FWD signals modifications (the modified part of the signal is marked as a red line).

Method no. 4: Signals registered using 1st method are filtered according to Eq. (1), assuming $n = 1$.

Method no. 5: Signals registered using 1st method are filtered according to Eq. (1), assuming $n = 5$.

Method no. 6: Signals registered using 2nd method are filtered according to Eq. (1) assuming $n = 1$.

Method no. 7: Signals registered using 2nd method are filtered according to Eq. (1) assuming $n = 5$.

Method no. 8: Referential method. $F(t)$ and $u_r(t)$ signals are not distorted in any way. A Classical Deflection Curve (CDC) construction with the commonly accepted standard ($F = F_{max}, u_r = u_{r(max)}$) is used.

In general, the analysis in the current study was conducted on a population of a dozen methods of source signal modification, reduced by a discrimination method to the eight discussed above.

3.2. Step two, fast Fourier transform operator

It is subsequently assumed that when consecutive values of $F(t)$ and $u_r(t)$ are calculated to 0 Hz frequency, the dynamic task is reduced to a static task (details of this approach are given by Guzina and Osburn (2002)). Deflection values normalised in this way can be used for building a new curve, which is named in this paper as a quasi-static deflection curve (in short QSDC). Transforming the signals to the frequency domain was performed using the discrete formula (2).

$$X(T) = \sum_{t=1}^n x(t)e^{(t-1)(T-1)(-2\pi i)/n} \quad T = 0, \dots, n \quad (2)$$

where:

n – number of elements,

$X(T)$ – signal in the frequency domain,

$x(t)$ – signal in the time domain.

The normalisation was limited exclusively to the frequency normalisations of particular $F(t)$ and $u_r(t)$ signals. It should be noted that whenever only backcalculation results are assessed, and not the direct values of pavement deflections, the recalculation of FWD measurement signals to the normalised force amplitude (e.g. 50 kN) does not add anything new to the analysis. The impact of frequency normalisation on the shape of a sample deflection curve is shown in Fig. 4.

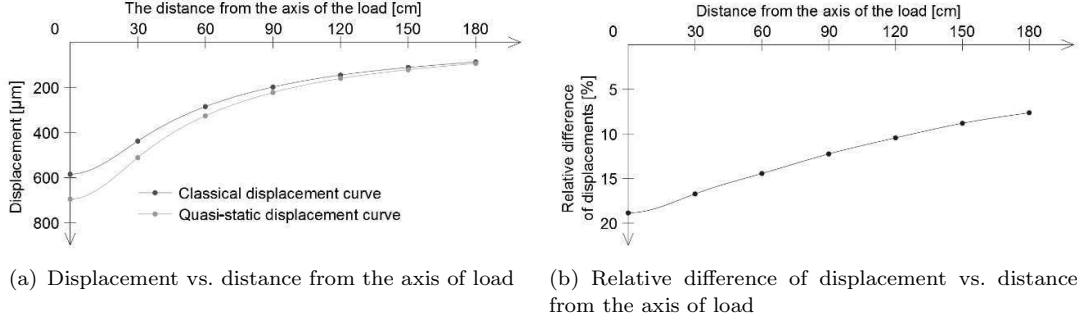


Figure 4. Comparison of the QSDC and CDC.

3.3. Uncertainty of a normalised signal

Using the frequency normalisation for the signals received in the FWD tests has an additional effect of limiting the influence of the measurement uncertainty related to both the frequency of the applied load and the frequency of medium's response. The conducted analysis assumes that systematic uncertainty of FWD measurements consists of two main factors: load determination uncertainty (equal to 2% of the searched value), and the deflection determination uncertainty (also equal to 2% of the searched value), as reported in FWD manual by Dynatest (2006). Considering that the uncertainty range equal to the statistical scatter of the determined displacement values can be expressed with $u = \bar{u} \pm 0.02 \cdot \bar{u}$ equation, where \bar{u} is the maximum registered displacement value in a given measuring point for a given condition. The load determination uncertainty and accidental uncertainty are disregarded. Generally, the vertical displacements caused by impact loads (such as in the case of FWD application), can be expressed with Eq. (3):

$$u_r(t) = f_r(F, \xi_F, T, E_i, \nu_i, h_i, p_i, w_i) \quad (3)$$

where:

t – time [s],

r – distance from the load axis marked in the horizontal plane [m],

F – load of pavement [kN],

ξ_F – frequency of loading signal [Hz],

T – temperature of the asphalt layers [$^{\circ}\text{C}$],

i – layer number,

E – elasticity/stiffness modulus [MPa],

ν – Poisson's ratio [-],

h – layer thickness [cm],

p – parameter defining the inter-layer bonding [-],

w – moisture [%].

When the analysis concerns a certain set of conditions, it can be assumed that (T , E_i , ν_i , h_i , p_i , w) values are constant. In consequence, Eq. (3) can be reduced to Eq. (4).

$$u_r(t) = f_r(F, \xi_F) \quad (4)$$

The influence of the coefficient of frequency on pavement deflections is omitted in classical analyses. In classical approach of backcalculation only maximum values of the force and displacement in time are usually considered. This is due to the fact that the frequency of the load in this type of measurement is about 20 Hz, which naturally gives rise to the assumption of negligible impact of inertial forces consequently leading to simplification of the analysis. It is demonstrated in this paper, inter alia, in relation to the ground GM, that low frequency load can also generate a significant statistical scatter of pavement backcalculation results. Thanks to the Fourier transform in the form of (5)

$$\hat{f}(\xi) = \lim_{T \rightarrow +\infty} \int_{-T}^T f(t) e^{-2\pi i x \xi} dx \quad (5)$$

both for $u(t)$ – displacement function as well as $F(t)$ – force function, Eq. (4) can be reduced to Eq. (6), assuming that the frequency of a given function is constant.

$$u_r(\xi) = f_r(F) \quad (6)$$

For example, let us assume that the displacement function $u(t)$ is expressed by Eq. (7),

$$u = \sin\left(\frac{t^2}{4}\right) \quad (7)$$

and the uncertainty range of determined deflections is described by Eq. (8).

$$u = \bar{u} \pm 0.02 \cdot \bar{u} \quad (8)$$

By substituting the values of time corresponding to the function's extremum in the place of t , it is possible to conclude that the uncertainty of the classical deflection curve is in the range of 1 ± 0.02 . Next, applying normalisation using the Fourier transform to Eq. (7), leads to the function $u(\xi)$ expressed with Eq. (9).

$$\hat{u}(\xi) = -\sqrt{\frac{\pi}{4}} \sin\left(\frac{\pi^2 \xi^2}{4} - \frac{\pi}{4}\right) \quad (9)$$

As the frequency of 0 Hz is equivalent to the condition without any dynamic influence, after substituting $\xi = 0$ to Eq. (9), determination uncertainty of the quasi-static deflection curve belongs to the interval of values in the range of $\hat{u}(\xi = 0) \cong 0.6387 \pm 0.01277$. It can be noticed that it is a narrower interval in comparison with the interval of the classical curve, that is 1 ± 0.02 , as shown in Table 1. Due to the linear nature of the transform, this conclusion is true for every amplitude and any combination of the function sum of Eq. (7).

Table 1. The determination uncertainty intervals for pavement deflections obtained using a classical and a quasi-static deflection curve.

	Classical deflection curve	Quasi-static deflection curve
Example of a deflection function	$u(t) = \sin\left(\frac{t^2}{4}\right) \pm 0.02 \cdot \sin\left(\frac{t^2}{4}\right)$	$\hat{u}(\xi) = -\sqrt{\frac{\pi}{4}} \sin\left(\frac{\pi^2 \xi^2}{4} - \frac{\pi}{4}\right) \pm 0.02 \cdot \left(-\sqrt{\frac{\pi}{4}} \sin\left(\frac{\pi^2 \xi^2}{4} - \frac{\pi}{4}\right)\right)$
The uncertainty interval for the maximum deflection value	1 ± 0.020	0.64 ± 0.013

4. Experimental section characteristics

The backcalculation were performed on the pavement whose structure and layers thicknesses are shown in ig. 5a and Fig. 5b, respectively.

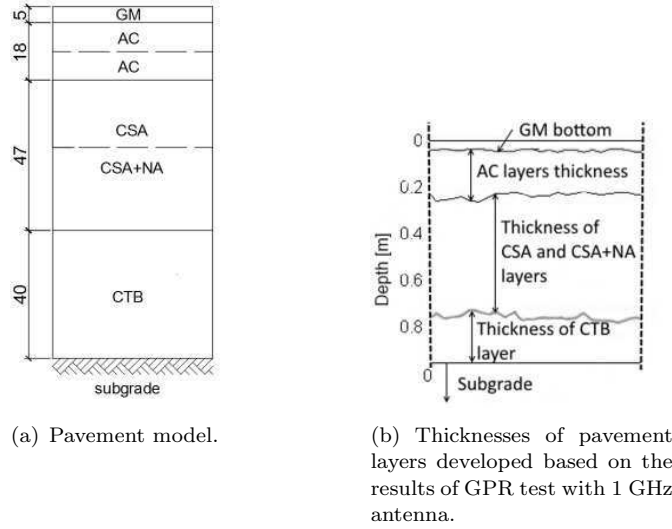


Figure 5. Pavement structure of experimental section.

The acronyms used in Fig. 5a, refer to the following layers: GM (Grouted Macadam), AC (Asphalt Concrete 0/22 mm), CSA (Crushed Stone Aggregate), CSA + NA (Crushed Stone Aggregate with Natural Aggregate 50/50%) and CTB (Cement Treated Base). Detailed changes and thickness fluctuations of pavement layers in the tested section were determined by a ground penetrating radar (GPR) equipped with an antenna of 1 GHz frequency. The results of the GPR tests were calibrated based on the thicknesses determined by drilling. The analysis of the results obtained from the GPR suggests that one should attribute different thicknesses to the layers in the models for each location where the pavement deflection tests were performed by means of the FWD method. In reference to the macroscopic assessment of cylindrical samples cut from the pavement, it is observed that, the cement grout did not penetrate the bottom of the AC layer (as one would expect), which meant that the interlayer bonding was tight enough.

FWD tests of pavement were performed on 57 measurement work stations. All the measurements were carried out on the surface of GM pavement layer. Nine loads (3x50 kN, 3x70 kN and 3x90 kN) were applied for each experimental point and the load and displacement functions in time were registered, as shown earlier in Fig. 1. Displace-

ments were registered both in the pavement load axis, as well as in the distances of 20, 45, 60, 90, 120, 150, 180 cm from the axis. For comparison, the laboratory tests using the method of indirect tensile modulus (ITSM) were also carried out (according to EN 12697-26 standard). Cylindrical samples for laboratory tests were cut from both GM surface layer and the two layers of AC. The values of elasticity moduli of cylindrical samples obtained by the indirect tensile tests are summarized in Table 2. The load frequency, determined based on the shape of the force impulse generated in a standard ITSM test amounts to $f = 0.25$ Hz and is calculated for a standard load increase time of 0.124 second.

Table 2. The values of stiffness E_{ITSM} , obtained from the method of indirect tensile modulus (ITSM).

Sample cut from layer	Temperature [°C]	Stiffness modulus [MPa]
GM	5	25 854
	7.5 ^a	23 700
	15	15 086
	25	9 185
AC	5	15 725
	7.5 ^a	14 267
	15	8 435
	25	3 494

^aInterpolated value

The results shown in Fig. 6, additionally confirm that the stiffness of samples cut from GM layer depends on the temperature (similarly to the features of samples from AC layers).

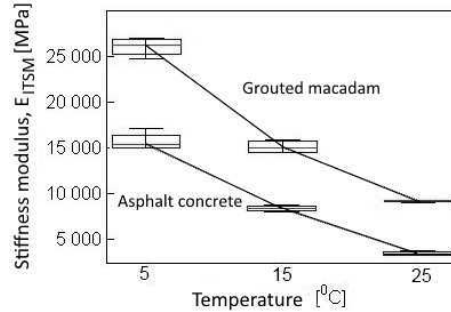


Figure 6. The stiffness modulus diagram $E(\text{Temperature}, f = 0.25 \text{ Hz})_{ITSM}$.

Therefore, the FWD measurements, on the pavements with the GM layer, need to be adjusted according to the temperature of the GM layer during measurements in situ.

5. Backcalculation of pavement with normalisation concept

In the analysed case, the bitumen-like features make an adjusting wearing course (GM) and binder course (AC) comparable; however the physical and mechanical properties differ at least in terms of dielectric constant, stiffness modulus and Poisson's ratio. For this reason, a model with a separate GM layer is further considered in the backcalculation. Unequivocal values of elasticity modulus, obtained by pavement backcalculation

methods, are only calculated on the assumption that the thicknesses of layers and type of the pavement are known. Attempts to weaken these assumptions can be found among others in (Garbowski & Pożarycki, 2016; Moshe, 2011; Saltan, Uz, & Aktas, 2013; Terzi, Saltan, Kucuksille, & Karasahin, 2013)

5.1. Backcalculation procedure

The backcalculation in a standard case is the process of searching for values of stiffness modulus (E_i) of the i^{th} -layer, so that the difference between pavement deflection curves calculated on the basis of a model and the measured values reaches the minimum. Taking the normalisation idea of the signals obtained during FWD tests into account, a standard backcalculation procedure is represented by the path of a block diagram (Fig. 7), described as a "classical displacement curve". For the procedure with signal normalisation (such as the one proposed in this paper), one needs to choose the path shown as a "quasi-static displacement curve" in Fig. 7.

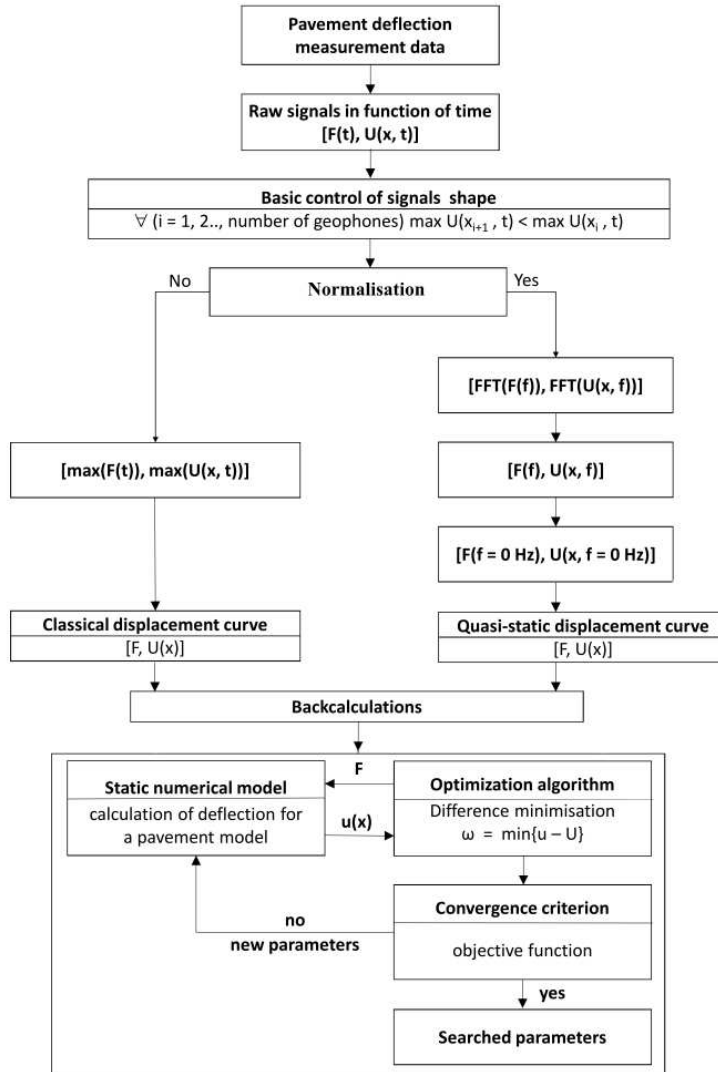


Figure 7. Backcalculation algorithm with the normalisation idea.

It needs to be mentioned that the area value with the correction factor (AVCF) formula, described in detail by (Pan, Sangghaleh, Molavi, Zhao, & Yi, 2012) was chosen as the optimising criterion, characterising the difference of adjustment between the deflection curves. Furthermore, Nelder-Mead's optimising algorithm (Yi & Mun, 2009) was used in the calculations and all results which failed to fulfil the $AVCF \leq 5\%$ are omitted in the final analysis.

5.2. Pavement models

The analysis of stiffness/elasticity moduli was performed based on the four independent pavement models (Fig. 8). Several models were applied to consider both the separation of the CTB layer from the subgrade (with a varying thickness for technological reasons) and the stiff layer in the model.

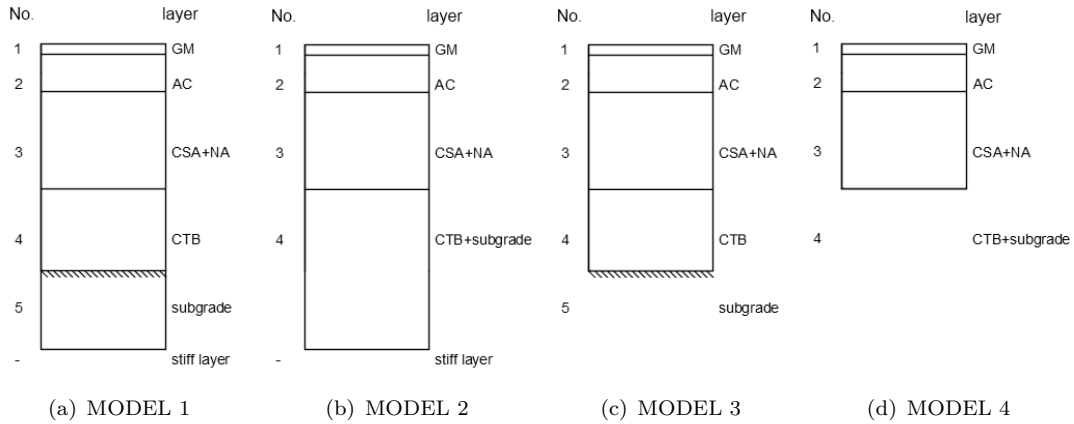


Figure 8. Pavement models with the grouted macadam layer.

The analysis with the stiff layer technique is also included with the reference to pavement backcalculation methods (shown as a stiff layer in Fig. 8). The adopted method of determining foundation depth B of the slab of the stiff layer with respect to the pavement surface is described by Rohde and Scullion (1990). The relationship for the discussed layer thicknesses (sum of AC and GM layers) was assumed according to Eq. (10). It should be noted that due to the empirical character of Eq. (10), all the calculations were carried out using the units used originally by Rohde and Scullion (1990).

$$\frac{1}{B} = 0.0409 - 0.5669r_0 + 30137r_0^2 - 0.0033BDI - 0.665\log(BCI) \quad (10)$$

where:

B – foundation depth of the rigid layer slab with respect to the pavement surface [foot],

r_0 – parameter whose value depends on the shape of the displacement curves controlled by Base Damage Index (BDI) and Base Curvature Index (BCI) values [mils]. The displacement curves were normalised to a 9 000 lb (40 kN) loading.

5.3. *Stiffness calculations*

The calculation results of stiffness/elasticity moduli for GM and AC layers of the pavement model are presented in Fig. 9. The obtained values are presented in the form of box-plots. The calculation results are shown for all eight FWD source signal modification methods numbered according to the description given in Section 3. Each box visually represents the descriptive statistics of calculated sample population for every combination model/method. The tops and bottoms of each box are the 25th and 75th percentiles of the samples. The distances between the tops and bottoms are the interquartile ranges. The whiskers are lines extending above and below each box. Whiskers are drawn from the ends of the interquartile ranges to the furthest observations within the whisker length. Observations beyond the whisker length are marked as outliers (a value that is more than 1.5 times the interquartile range away from the top or bottom of the box). Outliers are displayed with a red “+” sign. The line in the middle of each box is the sample median. If the median is not centred in the box, it shows sample skewness.

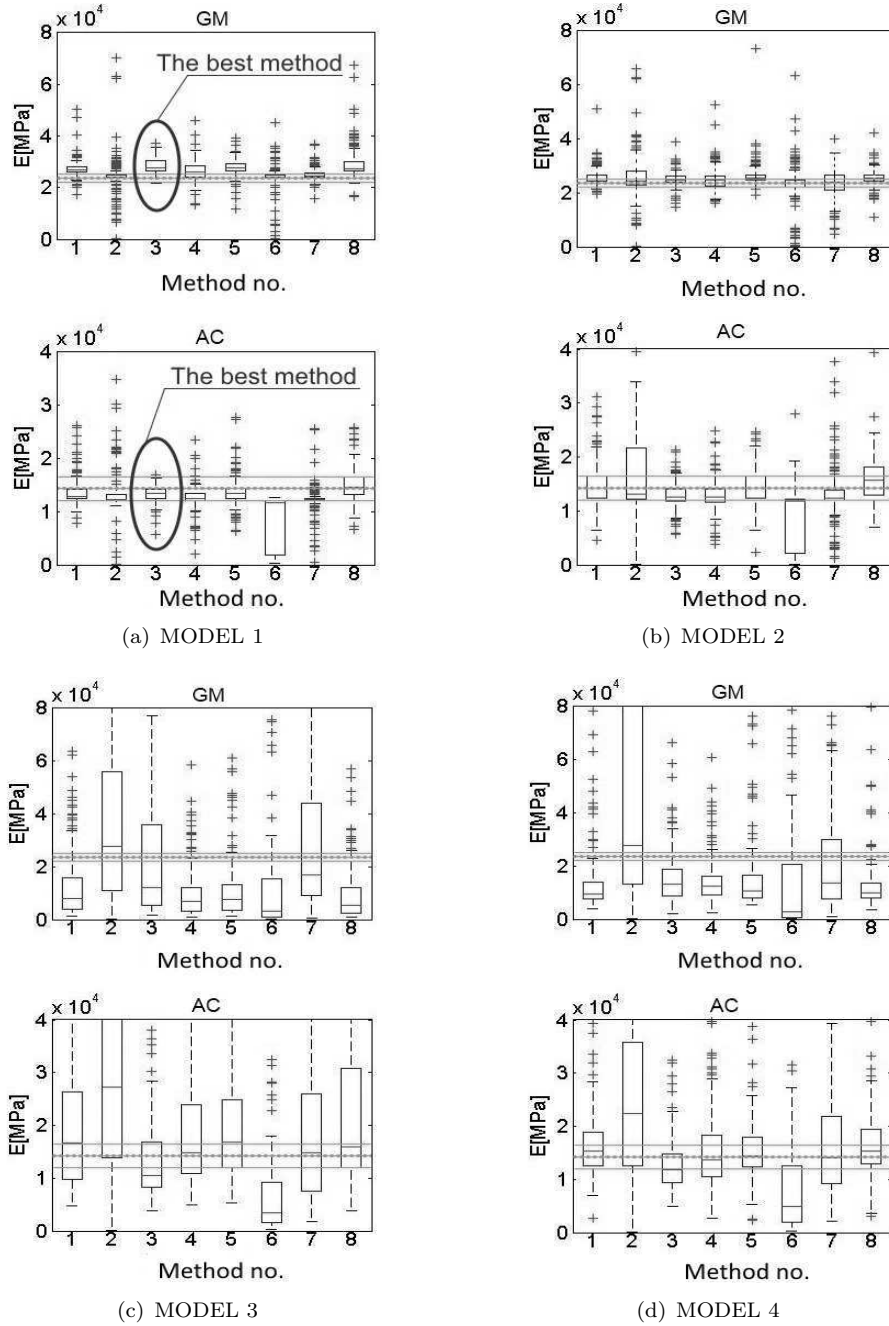


Figure 9. The stiffness/elasticity moduli determined for (green colour is used for marking both: average moduli \bar{E} and doubled standard deviation $\pm 2 \cdot \sigma_E$ values determined in laboratory following the ITSM method.

The statistical scatter of the elasticity/stiffness moduli calculation results for both QSDC and CDC methods and selected pavement models was also assessed using a scatter measure expressed with the coefficient of variation (Cv). The computed values of Cv are presented in Table 3. The values marked with the bold font are the results for the best configuration model/method.

Table 3. Coefficients of variation describing the statistical scatter of the backcalculation results.

$Cv[-]$	Number of pre-processing method according to Section 3 description							
	1	2	3	4	5	6	7	8 (CDC) ^b
	MODEL 1							
Cv_{GM}	1.343	0.8285	0.0997^a	0.1482	0.1211	0.2635	0.0983	0.2139
Cv_{AC}	0.2010	0.1215	0.1117^a	0.1920	0.2017	0.6675	0.2197	0.2014
\overline{Cv}^c	0.7720	0.4750	0.1057^a	0.1701	0.1614	0.4655	0.1590	0.2077
	MODEL 2							
Cv_{GM}	0.1188	0.7238	0.1057	0.1853	0.1727	0.7493	0.2257	0.1188
Cv_{AC}	0.2682	1.6824	0.1897	0.2270	0.2424	1.1756	0.4084	0.3035
\overline{Cv}	0.1935	1.2031	0.1477	0.2062	0.2076	0.9625	0.3171	0.2112
	MODEL 3							
Cv_{GM}	1.1367	1.7507	1.1855	1.1515	1.0462	2.2395	1.2938	1.5630
Cv_{AC}	0.7570	5.1199	0.6590	0.6385	0.6469	3.6702	1.5667	0.5808
\overline{Cv}	0.9469	3.4353	0.9225	0.8950	0.8466	2.9549	1.4303	1.0719
	MODEL 4							
Cv_{GM}	0.8532	2.5593	0.6409	0.6142	0.8384	3.1400	1.5406	1.1542
Cv_{AC}	0.3882	1.2986	0.4291	0.4982	0.3718	1.9854	0.6128	0.3923
\overline{Cv}	1.9290	1.9290	0.5350	0.5562	0.6051	2.5627	1.0767	0.7733

^aCoefficients of variation values obtained for the most reliable backcalculation results

^bValues obtained for standard backcalculation procedure

^cThe mean value calculated as $(Cv_{GM} + Cv_{AC})/2$

The mean stiffness/elasticity moduli determined by the ITSM method and the backcalculation results bearing the lowest uncertainty are compared in Table 4.

Table 4. The stiffness comparison for results obtained only for MODEL 1 and Method 3).

Warstwa	$E_{ITSM} \pm 2\sigma$ [MPa]	$E_{backcalculated} \pm 2\sigma$ [MPa]
GM	23700 \pm 1279	28476 \pm 5280
AC	14267 \pm 1588	13201 \pm 2640

Considering model 1 and method 3 as the most reliable in this type of structure (Fig. 9a), the value obtained in backcalculation was 20% larger than that from the laboratory tests when GM layer was taken into account. In the case of AC layer backcalculated value was 7% less than that determined in the laboratory.

6. Discussion

A deflectometer device, which provides measurements of the displacement accuracy of ± 2 micrometers was used in the study. However, the paper focuses solely on identifying the elasticity modulus value using the backcalculation method for the pavement which although has the thin layer (GM), but its stiffness at a given temperature is significantly larger when compared to its adjacent layer made of AC ($E_{AC} = 15000$ MPa $>$ $E_{GM} = 25\,000$ MPa for $T = 15^\circ\text{C}$). Introducing the backcalculation procedure with the curve normalisation, the authors try to first eliminate the influence of excessive tendency of thin layers to oscillate under the impact load that acts on the pavement. Further, it is noted that in spite of the relatively low frequency of the impact load function (≈ 20 Hz), influence of the discrepancies between the results of which are derived from dynamic testing, and the results of the backcalculation performed by using the static

pavement model, obtained without the normalisation described in the article are practically useless. Unreasonably large statistical scatters which are presented graphically in the form of red markers "+" in Figure 9 justify such a conclusion.

Based on the calculation and analysis carried out in this study, it was observed that in comparison to the benchmark method (i.e. the standard backcalculation procedure), methods no. 3, 4 and 5 reduced the statistical scatter by 24.4, 19.3 and 19.5%, respectively. However, for methods no. 1, 2, 6 and 7, the statistical scatter increased by 11.8, 211.1, 206.7 and 31.7%, respectively, compared to the standard backcalculation method. Depending on the applied calculation model the statistical scatter for methods no. 4 to 7 is characterised by either a higher or lower value of the coefficient of variation, in relation to the benchmark value. Anyway, slight inconvenience of source signal modification using Eq. (1) (that one with n parameter) deals with the fact that the results obtained in the form of elasticity moduli of the pavement model layers, depend to a great extent, on the applied value of the n parameter. The factor in question affects the determination of stiffness. Having in mind that backcalculation results are assumed for the scatter measure, the values of the coefficient of variation shown in Table 3 prove that the smallest scatter relates to those model application variants in which the stiff layer has been defined (models 1 and 2). When the same measure was applied to the selected pre-processing methods of the analysed signals, the smallest scatter was achieved for method no. 3. However, it is worth noting that the scatter of around 10% obtained for model no. 1, is typically acceptable for engineering design of pavement overlays. Additionally, the smallest scatter and obtained values of elastic moduli are in the acceptable range of values obtained from the laboratory tests (where range is the distance between the top and bottom of green lines drawn in Fig. 9).

For the sake of limiting the statistical scatter, method no. 3 appears to be the best solution out of all considered proposals. This method enables one to determine sets of values for elasticity/stiffness moduli, in which the statistical scatter for all models is lower by approximately 24.4%, in comparison with the benchmark backcalculation method. Considering only those backcalculation results which modelled the pavement following the concept called MODEL 1, the statistical scatter of backcalculated moduli values was reduced by 49.1% in comparison with the benchmark method.

The elasticity/stiffness modulus calculated using the QSDC is characterised by lower values than those obtained from backcalculation using the CDC, which is a desired symptom. The QSDC approach corresponds to the lower frequency than that of the CDC. For typical pavement AC – like materials, the lower frequency of load results in the lower value of the elastic modulus. This relationship had been recognized for most methods and models of stiff layers. Moreover, using a GPR for the detection of a constructed pavement layer system is often inadequate for determining the boundaries of between asphalt courses. Whenever the adjusting courses are GM and AC layers, the analysis of GPR test results for the pavement allows establishing those boundaries unambiguously. Interestingly, the analysis of GPR test results showed that the separation of the grouted macadam layer out of the asphalt layers was possible using the device equipped with an antenna of 1 GHz frequency. It is well known that such analysis cannot be carried out for two adjacent AC layers because their identification on the radargram obtained from the pavement test performed with the GPR device equipped with the antenna of 1 GHz frequency is not possible. Therefore, the GPR results presented in this paper may be regarded as the first step confirming the logic of separating independent GM and AC layers in the pavement model for the backcalculation of pavements.

7. Conclusions

The results of the backcalculation performed for grouted macadam pavement displacement values obtained from the FWD device are presented and analysed in this paper. It can be concluded that whenever one of pavement courses is substituted with a 5cm thick grouted macadam layer, the system created in this way classifies as one with the thin layer. The analysis presented in this paper confirms that determining the stiffness of pavement layers using a model with a separate thin grouted macadam layer is possible, and using frequency normalisation of the load function and the pavement response enables one to limit the statistical scatter of the backcalculation on a uniform pavement section by 49%.

In reference to eight representative methods of modifying force and displacement signals from pavement deflection measurements, the smallest scatter was achieved by means of method where FWD signal values oscillating very closely to the argument axis were assumed to be zero. The scatter of backcalculated moduli values around 10% applies exclusively to the model resembling very closely the system of the real pavement. Introducing a stiff layer and modifying source signals of force and displacements with the best method, confronted with the results of laboratory tests, suggests strongly that when a static pavement model is used for dynamic test analysis, a normalisation method increases the reliability of backcalculation results. The work presented in this paper also confirms the suggestions formulated by other authors that the values of stiffness moduli backcalculated for a layer model made of asphalt concrete are lower than those determined in the laboratory using the indirect tensile method (Shalaby, Liske, & Kavussi, 2004). For values of stiffness moduli backcalculated for a layer model made of grouted macadam there is an inverse relationship. The difference between mean values of backcalculation results and laboratory tests results obtained for AC samples, amounts to around 7%. In the case of courses made of grouted macadam, the calculated values of stiffness moduli are higher than those obtained from the laboratory tests, and the difference between the mean values from the backcalculation and experiments is equal to 20%.

Finally, it is worth pointing out that it is possible to identify in-situ two adjacent layers made of the grouted macadam and the asphalt concrete based on the radargrams obtained from the GPR device equipped with a 1 GHz antenna. This proves that the grouted macadam layer is characterised by a different value of dielectric constant compared to the course made of asphalt concrete.

Funding This work has been partially supported by the Polish National Centre for Research and Development Grant No. 244286 entitled ‘Precise system of the load capacity parameters identification of roadway structure in predicting the lifetime of road pavements’.

References

- Al-Khoury, R., Scarpas, A., Kasbergen, C., & Blaauwendraad, J. (2001). Spectral element technique for efficient parameter identification of layered media. part i: Forward calculation. *International Journal of Solids and Structures*, *38*, 8753-8772.
- Al-Qadi, I. L., Wang, H., & Tutumluer, E. (2010). Dynamic analysis of thin asphalt pavements by using cross-anisotropic stress-dependent properties for granular layer. *Journal of the Transportation Research Board*, *2154*, 156-163.
- Anderton, G. (2000). *Engineering properties of resin modified pavement (RMP) for mechanistic*

- design* (Tech. Rep.). US Army Corps of Engineers. Engineer Research and Development Center.
- Bianchini, A. (2014). Thin asphalt pavement performance equation through direct computation of falling weight deflectometer-derived strains. *International Journal of Pavement Engineering*.
- Ceylan, H., Gopalakrishnan, K., Bayrak, M. B., & Guclu, A. (2013). Noise-tolerant inverse analysis models for nondestructive evaluation of transportation infrastructure systems using neural networks. *Nondestructive Testing and Evaluation*, 28, 233-251.
- Collop, A. C., & Elliott, R. C. (1999). Assessing the mechanical performance of densiphalt. In *3rd european symposium on the performance and durability of bituminous materials and hydraulic stabilised composites*.
- Dynatest. (2006). Dynatest FWD/HWD test systems and owners's manual version 2.0.0 [Computer software manual].
- Garbowski, T., & Pożarycki, A. (2016). Multi-level backcalculation algorithm for robust determination of pavement layers parameters. *Inverse Problems in Science and Engineering*, 0(0), 1-20. Retrieved from <http://dx.doi.org/10.1080/17415977.2016.1191073>
- Guzina, B. B., & Osburn, R. H. (2002). Effective tool for enhancing elastostatic pavement diagnosis. *Transportation Research Record 1806 Paper No. 02-3196*.
- Irwin, L., Yang, W., & Stubstad, R. (1989). *Deflection reading accuracy and layer thickness accuracy in backcalculation of pavement moduli*. American Society for testing and Materials.
- Kang, Y. (1998). Multifrequency back-calculation of pavement-layer moduli. *Journal of Transportation Engineering*, 124, 73-81.
- Moshe, L. (2011). An alternative forwardcalculation technique as a screening procedure for review and evaluation of backcalculated moduli. *International Journal of Roads and Airports (IJRA)*, 1(2), 85-117.
- Oliveira, J. (2006). *Grouted macadam – material characterization for pavement design* (Unpublished doctoral dissertation). University of Nottingham.
- Oliveira, J., Salah, Z., Thom, N., & Pereira, P. (2007). A simple approach to the design of pavements incorporating grouted macadams. In *4th internacional conference bituminous mixtures and pavements*.
- Pan, E., Sangghaleh, A., Molavi, A., Zhao, Y., & Yi, P. (2012). *An efficient and accurate genetic algorithm for backcalculation of flexible pavement layer moduli* (Tech. Rep.). The University of Akron.
- Papadopoulos, E., & Santamarina, J. (2015). Analysis of inverted base pavements with thin asphalt layers. *International Journal of Pavement Engineering*.
- Rohde, G., & Scullion, T. (1990). *Modulus 4.0: Expansion and validation of the modulus backcalculation system* (Tech. Rep.). Texas Transportation Institute.
- Saltan, M., Uz, V. E., & Aktas, B. (2013). Artificial neural networksbased backcalculation of the structural properties of a typical flexible pavement. *Neural Computing and Applications*, 23, 1703-1710.
- Sangghaleh, A., Pan, E., Green, R., Wang, R., Liu, X., & Cai, Y. (2013). Backcalculation of pavement layer elastic modulus and thickness with measurement errors. *International Journal of Pavement Engineering*, 15(6), 521-531.
- Setyawan, A. (2006). Assessing the compressive strength properties of semi-flexible pavements. In *The 2nd international conference on rehabilitation and maintenance in civil engineering*.
- Shalaby, A., Liske, T., & Kavussi, A. (2004). Comparing back-calculated and laboratory resilient moduli of bituminous paving mixtures. *Canadian Journal of Civil Engineering*, 31(6), 988-996. Retrieved from <http://dx.doi.org/10.1139/104-065>
- SHRP. (1993). *Sharp's layer moduli backcalculation procedure* (Tech. Rep.). Strategic Highway Research Program.
- Terzi, S., Saltan, M., Kucuksille, E. U., & Karasahin, M. (2013). Backcalculation of pavement layer thickness using data mining. *Neural Computing and Applications*, 23(5), 1369-1379.
- Ullidtz, P., & Coetzee, N. F. (1995). Analytical procedures in NDT pavement evaluation. In *Transportation research record no. 1482 (july 1995)*.

- Von Quintas, H., Bush, A., & Baladi, G. (Eds.). (1994). *Nondestructive testing of pavements and backcalculation of moduli: Second volume*. ASTM International.
- Von Quintas, H., & Killingsworth, B. (1997). *Design pamphlet for the backcalculation of pavement layer moduli in support of the 1993 AASHTO guide for the design of pavement structures* (Tech. Rep.). U.S. Department of Transportation. Federal Highway Administration.
- Westover, T., & Guzina, B. (2007). Engineering framework for the self-consistent analysis of FWD data. *Transportation Research Record*, 55-63.
- Wozniak, M. (1996). 2d dynamics of a stratified elastic subsoil layer. *Archive of Applied Mechanics*.
- Yi, J. H., & Mun, S. (2009). Backcalculating pavement structural properties using a Nelder–Mead simplex search. *Int. J. Numer. Anal. Meth. Geomech*, 33, 1389–1406.